Development of the Numerical Model of the New-born Child Dummy Q0

Christian Gehre, Prof. Volker Schindler
Technical University of Berlin, Germany

Abstract:

The European research project "CHILD" (Child Injury Led Design) is working on the improvement of passive safety of children as occupants in cars. One of the objectives is to develop new child dummy models. This paper focuses on the development of the finite element model of the new-born child dummy Q0 for the use with LS-Dyna.

The Q0 model was created by using the CAD models of the hardware-Q0. All non-rigid body segments such as head, neck and torso were validated by using results of component tests. Optimisation tools were used to identify the adequate material models for the body segments and to define the parameters of these materials.

The response of the dummy database in the calibration test procedures correlates well with the physical Q0 dummy. Furthermore, all parts would pass the certification requirements.

Keywords:

Passive safety, validation, dummy, new-born child dummy, Q dummy series

1 Introduction

The new-born child dummy Q0 (Figure 1), developed by TNO and FTSS was one of the first results of the "CHILD" project. The numerical model is based on this first series of Q0 dummies. It represents a six week old infant with a mass of 3.4 kg and a sitting height of 355 mm. The Q0 was designed for the use with child restraint systems (CRS) group 0/0+ in frontal, lateral, rear and roll-over crash configurations.

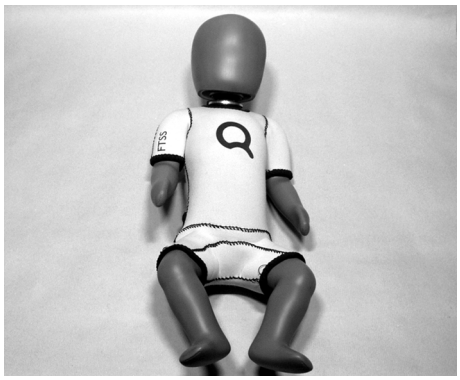

Figure 1: Child dummy Q0.

Compared to the P0 and the CAMI dummy, the Q0 offers the opportunity to measure head, chest and pelvis accelerations as well as the upper neck forces and torques. So it is now possible to assess the protection level of child restraints of this age group by using physical measurements on the dummy.

2 Method

Those parts of the dummy, which are designed to be non-deformable in a crash test, are made as rigid bodies in the model to reduce the total computing time. All other parts of the model, such as skin of the head, rubber of the neck or torso foam are using non-rigid materials to describe the material behaviour of these dummy parts. All non-rigid parts were validated by using results of component tests with these parts or an assembly with these parts involved. The torso foam was validated by using results of thorax impact tests with the complete dummy. These tests cover a wide range of loads to the dummy. So the risk of a validation to only one load condition was significantly reduced.

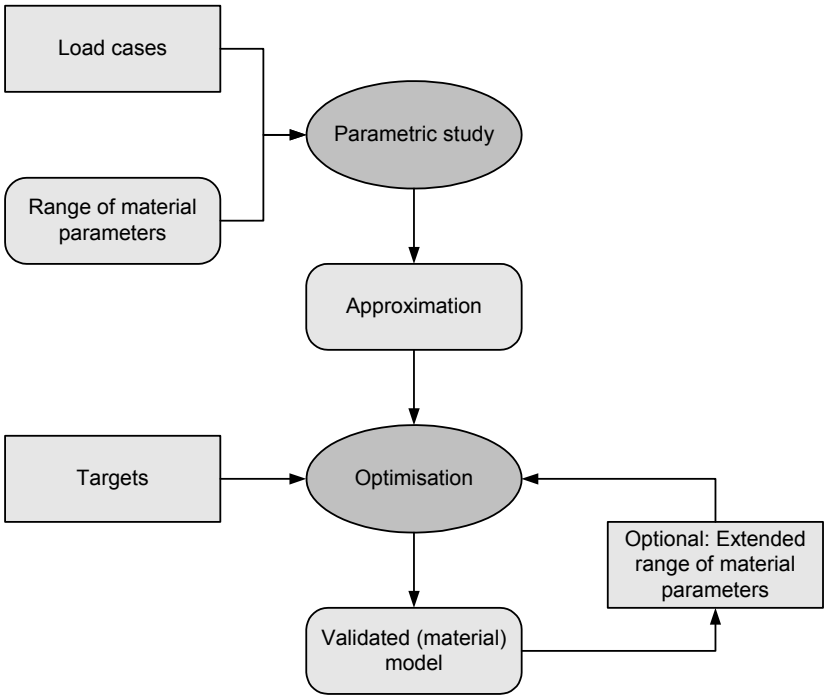

Figure 2: Structure of parametric study and optimisation process.

Figure 2 shows the method used to validate the dummy model in principle. In a first step of the validation, appropriate material models were pre-selected for the validation process. Secondly, the material models were roughly pre-validated manually to limit the range of the material parameters. Afterwards the pre-validated model with all load cases of one test set-up was included in Altair Hyperstudy. So, for instance all three load cases of the head drop tests were analysed at the same time.
Within Hyperstudy a full factorial parametric study was started for every pre-selected material or, if different FE-meshes were analysed, for every mesh. One of the results of such a study are interactions between the different material parameters and the model's response.
Based on the results of the parametric study a mathematical approximation of the model was automatically created. It was the base of the optimising tool, which tried to adapt the parameters to get the best response of the model. Afterwards the optimisation routine was restarted with the parameters optimised in the previous step. A much better response of the model was so achieved in most of the cases.
The finally selected material parameters such as Young's modulus do not necessarily correlate with the physical value. They are also influenced by other parameters of the model such as size of the mesh.

3 Structure of the dummy model

Figure 3 shows the Q0 dummy model. It has a skull, a neck, a rigid thoracic spine, a lumbar spine, which is identical to the neck, and a rigid pelvis. The torso part, made of foam, covers the internal structure of the dummy from the pelvis up to the shoulders. The bent arms and legs are directly screwed to the upper thoracic spine and the pelvis, respectively. Their only degree of freedom is the rotation around the transverse axis. A neoprene suit covers the torso as well as upper arms and legs.

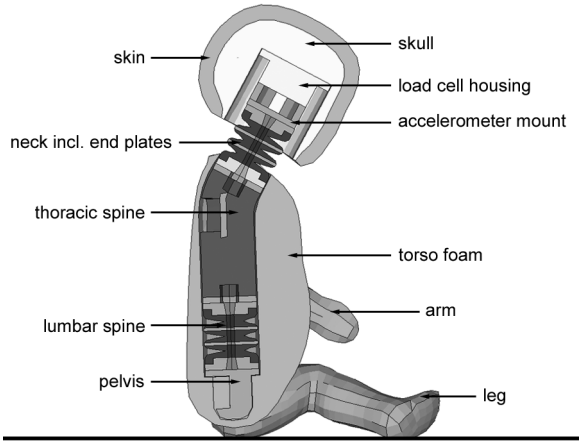

Figure 3: Structure of the Q0 dummy model.

The FE-mesh of all parts is made of solid elements, mainly of six-node hexagon and five-node pentagon elements. The surface of some parts is covered with a thin layer of shell elements. It is used as interface for contacts to other parts of the dummy and the surrounding areas. In total 7,100 nodes, 1,700 rigid elements and 10,600 deformable elements are used for the dummy.

The dummy model was developed and validated for the use with the finite element solver LS-Dyna 970, release 3858.
The total computing time of the dummy without any environment, such as CRS, is approximately 13 seconds for every millisecond of simulation time on a Pentium 4 3.0 GHz machine.

3.1 Head

The head assembly is made of skull including skin layer, upper neck load cell and accelerometer mount. A non-linear visco-elastic material model was used for the skin and an elastic material for the beam of the load cell. This beam connects the skull to the load cell housing. Skull, load cell housing and accelerometer mount are made of rigid material.

The head assembly includes a tri-axial accelerometer at the head's centre of gravity and a six-axial load cell to measure forces and torques in the upper neck of the dummy.

3.2 Neck and lumbar spine

The structure of the neck is similar to the neck of Hybrid III dummies. The main part, the neck mould, is made of rubber and includes two metal intermediate disks and is bounded by two end plate. A non-pre-tensioned steel cable, fixed between the two end plates, restricts the neck tension. Three slits at the front side of the neck mould are reducing the stiffness in extension bending.

The upper neck forces and torques are not measured at the occipital condyles (OC). Therefore, they must be corrected with the shear force, to obtain the response at the OC-joint. The equations to calculate these moments are shown in (1), (2) and (3).

$$M_{xOC} = M_x + 0.033 \cdot F_y \quad (1)$$

$$M_{yOC} = M_y - 0.033 \cdot F_x \quad (2)$$

$$M_{zOC} = M_z \quad (3)$$

The comparatively small and soft neck is very sensitive against the density of the used mesh. Some important geometrical details, such as the geometry of the slits, are lost by using a wider FE-mesh. The used fine mesh is a compromise of computing time, numerical stability and response of the upper neck load cell in the validation tests. In total six FE-meshes of different levels of detail were validated in parallel. Finally, one of the more simple meshes was chosen, because of its good responses in the validation tests and the short computing time.

The lumbar spine joint is identical to the neck assembly. It is mounted in upside down position with slits to the back of the dummy.

3.3 Thoracic spine and pelvis

The thoracic spine is made of rigid material. A tri-axial accelerometer measures the chest acceleration. The pelvis of the dummy is made of steel. So rigid material has been used in the model. It is equipped with a tri-axial accelerometer.

3.4 Torso and rubber suit

The torso flesh foam covers the skeleton of the dummy from the shoulders to the pelvis. It has a cut on the rear side from the upper pelvis to the lower neck to allow the assembly of the dummy. The cut is closed by the suit of the dummy.

Solid elements are also used for the torso part, but compared to the others, the solid mesh consists only of tretrahedron elements. The torso foam is fixed to the dummy's skeleton only by using contacts. No node or element is attached to another part of the dummy.

The Q0 dummy is provided with a suit, which covers torso, upper arms and uppers legs. The suit is not only necessary because of the additional soft layer on the dummy's surface, it also covers the gaps between extremities and torso.

4 Test procedures for the validation

Head and neck have to pass several certification tests [6] to show the biofidelity and to get the approval for the use in crash tests. Results of these tests were used to validate the model. Furthermore, some additional component tests with neck, torso and extremities, and thorax impact tests with the complete dummy were performed to obtain more data for the validation.

4.1 Head

The head assembly was validated by using three different set-ups of head drop tests (Table 1). Both tests with drop height of 130 mm are the certification procedure. The third one, a 45° frontal impact test with a drop height of 376 mm, is taken from the certification procedures of the 12 month old child dummy of the CRABI-series [1].

Not only the maximum head acceleration was used to validate the model of the head assembly. Also the shape of the acceleration curve should correlate with the experiment. The width of the signal is also described by the a_{3ms} value. So it was used as secondary parameter for the validation.

Table 1: Set-up of head validation tests.

Impact direction	Drop height	Angle
frontal	130 mm	28°
lateral	130 mm	35°
frontal	376 mm	45°

The maximum resultant head acceleration has to be between 91 g and 157 g in frontal and 94 g and 162 g in lateral direction to pass the certification requirements [6].

4.2 Neck

Two different test set-ups were used to validate the head-neck assembly in flexion, extension and lateral bending mode. In all lateral bending tests the head was mounted on the neck rotated by 90° around the vertical axis (rearward position) in order to have symmetrical neck loading.
In the first configuration the neck was mounted on a sled, which was accelerated by a pneumatic catapult. The second configuration, a pendulum test, is the certification procedure. The pendulum is described in Part 572 subpart E [2]. Figure 4 shows the average crash pulses of the pendulum and the sled tests. The average impact velocity was about 3.37 m/s in the pendulum tests and 4.12 m/s in the sled tests.

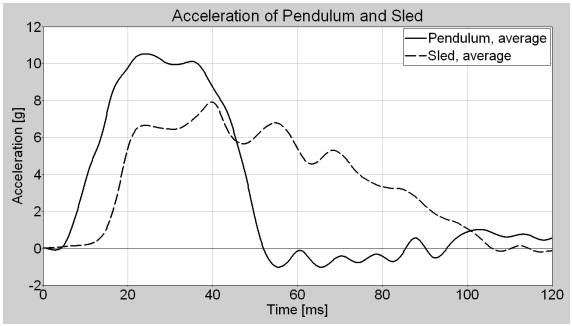

Figure 4: Acceleration in sled and pendulum tests.

The head rotation angle, the upper neck forces and torques were used as main target values to validate the model. Additionally the neck moment at the occipital condyles (OC-joint) was used. It is a simplified indicator of a correct time dependent course of neck forces and moments.

4.3 Torso foam

The torso was validated by using results of two different test set-ups. Firstly, a simple drop test was used to pre-validate the model and secondly, a thorax impactor test with the complete dummy for the final validation. A simulation run of a single thorax impact test using the complete dummy is, compared to all other validation tests, computationally expensive. So the drop test was used to make a quick pre-selection of the material model and the range of variation of material parameters. Thus, it was possible to reduce the total time of validation of the torso foam. The final validation of the foam was done with the complete dummy including all functions such as internal contacts and the attachment of the extremities to the skeleton with joints.
The mass of the impactor was about 2.6 kg and the impact velocity was 2.2, 3.2 and 4.3 m/s. Based on the longitudinal accelerations of chest and impactor the maximum chest deflection and impact force were calculated. Both parameters were used for the validation of the torso foam. The torso drop tests were performed with the same velocities as in the impactor tests.

4.4 Extremities

The extremities are not included in the certification procedures of the Q0. Therefore simple drop tests with different impact velocities, taken from the torso tests, were performed to obtain data to validate arms and legs of the model. Arm and leg were fixed with tape with their inner side under a steel plate of the test rig. So the load was applied to the parts in lateral direction. Following the validation of the head, peak and clip values of the impactor acceleration were used as main parameters of the validation.

5 Results

The sign conventions of the SAE J211 standard are used in the experiments and simulations for all measured values. Also all plots of these measures follow this standard.
All results, given in this paper represent a newer version of the dummy model, than described in [4].

5.1 Head

The head assembly was validated by varying the material model and the material properties of the skin layer of the head. All used material models have a visco-elastic characteristic. Finally MAT_062, a non-linear viscous foam was selected for the skin. The response of the tested linear material models could not be adjusted to the different impact velocities as exact as the non-linear model.

The ratio between head acceleration in the frontal and in the lateral impact test with a drop height of 130 mm was the main problem in the validation. It has to be approximately 1.05, but finally 0.94 was achieved with MAT_062, the best compromise of all tested materials.

Table 2. Maximum head acceleration.

Set-up	Experiment	Simulation
frontal, 28°, 130 mm	116.6 g - 122.8 g, av. 120.0 g	107.3 g
frontal, 45°, 376 mm	237.0 g - 276.3 g, av. 254.9 g	273.9 g
lateral, 35°, 130 mm	110.6 g - 116.7 g, av. 114.1 g	113.7 g

However, the maximum head acceleration as well as the a_{3ms} value correlate well with the experiment. Table 2 shows the maximum head acceleration of the finally selected and optimised viscous foam MAT_062. So the model fulfils the requirements of the certification tests.

The parameters influencing the maximum head acceleration are the initial Young's modulus (E_1) and the exponent in power law for Young's modulus (n_1) [5]. Declining E_1 and/or n_1 reduce the maximum head acceleration. In this case the a_{3ms} value increases. The influence of E_1 and n_1 increases with the impact velocity. Except for the Poisson's ratio, which has only a slight influence on the head response, all other parameters of MAT_062 have in principle the same behaviour as E_1 and n_1.

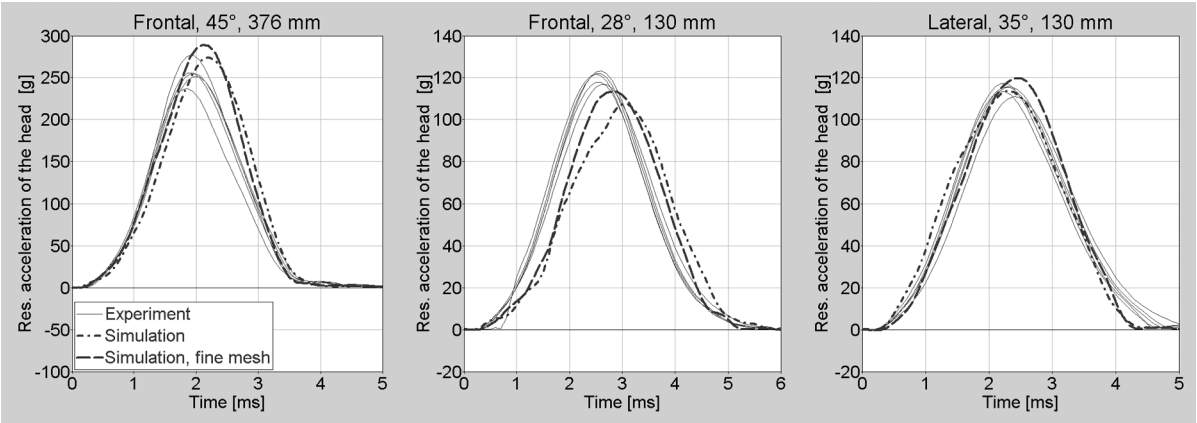

Figure 5: Head response in head drop tests.

Figure 5 shows the acceleration curves of experiments and simulation. The gradient of the acceleration in the model is lower than in the test in the 28° frontal impact configuration. Additional simulations using

MAT_062 and a mesh of smaller elements improved the shape of the curve, especially between 1.5 and 3.0 ms. At the same time the gradient of the declining edge gets slightly too high. A fine mesh generally stiffens the material, and the maximum acceleration increases.
The effect of stiffening the material to improve the shape of the curve affects also the other tested configurations. The shape of the head acceleration curve in the 45° frontal impact and the 35° lateral impact correlates better with results of the experiments than in the 28° frontal impact.
However, the achieved results already show a good agreement with target values of the experiments. Modifications of the skin's mesh could improve the shape of the acceleration curves. Therefore in a next step the mesh of the skin will be modified and the material parameters will be adapted to this new mesh.

5.2 Neck

The model was validated by varying the type of visco-elastic material of the neck rubber, the material properties of neck rubber and steel cable, the thickness of the contact between the neck segments and level of detail of the FE-mesh. MAT_006, a simple linear visco-elastic material model, was finally selected for the rubber parts of the neck. Other, more detailed visco-elastic materials of LS-Dyna offer more parameters to adapt the material in detail, but they had no advantage in this application. Furthermore the computing time of the neck was rather high when using these materials.

There are four parameters available in MAT_006, the elastic bulk modulus (BULK), a short-time (G0) and a long time (GI) shear modulus and finally the decay constant (BETA). Not all of them have the same effect on upper neck shear force, bending moment and head rotation angle.
The angle in all three loading configurations is mainly affected by the long-time shear modulus. An increasing GI reduces the head angle. The shear force is mainly influenced by G0 and BETA. They have opposite influence. An increasing G0 or a decreasing BETA are increasing the absolute shear force. The bending moment is mainly influenced by G0 and GI in extension bending and by BULK in flexion and lateral bending. Increasing BULK and G0 reduce and an increasing GI rises the measured torque.
A thick contact area reduces the bending angle of the neck, but it also has an influence on the moments. The torque is increasing under flexion bending and decreasing under extension bending with a thicker contact area.

MAT_001, an elastic material was chosen for the steel cable of the neck. The only varied influence parameter was Young's modulus E. Modifications of the cable stiffness affects mainly the rotation angle of the head, especially in the pendulum tests. A stiffer cable material reduces the angle. The Young's modulus of the cable was only varied in the neck pendulum test set-up.

The structure of the FE-mesh of the neck is an important parameter for the overall performance of the neck model. Figure 6 and Figure 7 are showing results of different levels of details. The less detailed mesh (Simulation 1) is more than 25% faster than the more detailed mesh (Simulation 2) by keeping the same response characteristic.

5.2.1 Neck sled tests

First of all the neck was validated by using the results of the sled tests. Afterwards the material properties were slightly adapted to also fit to the pendulum tests. Figure 6 shows the neck moment at the OC-joint versus the head rotation angle in all three bending modes, validated in sled and pendulum tests.

The model of the neck was validated by using the same priority of flexion, extension and lateral bending. So the validated model is a well balanced compromise.
The response of the neck in extension bending and lateral bending correlates well to the experiments up to a head angle of approximately 40°. The moment at the OC-joint is slightly too high in both load cases.
The neck is slightly too stiff in the flexion bending mode, but there already is a good correlation of simulation and experiment. The peak at an angle of 7° in the rebound phase of the neck is coming from the shear force signal and is probably caused by contact problems of the neck and the neck cable. This

phenomenon also occurred in simulations with a higher pulse, but disappears when using a softer cable. However, in none of the simulations any element of the neck collapsed.

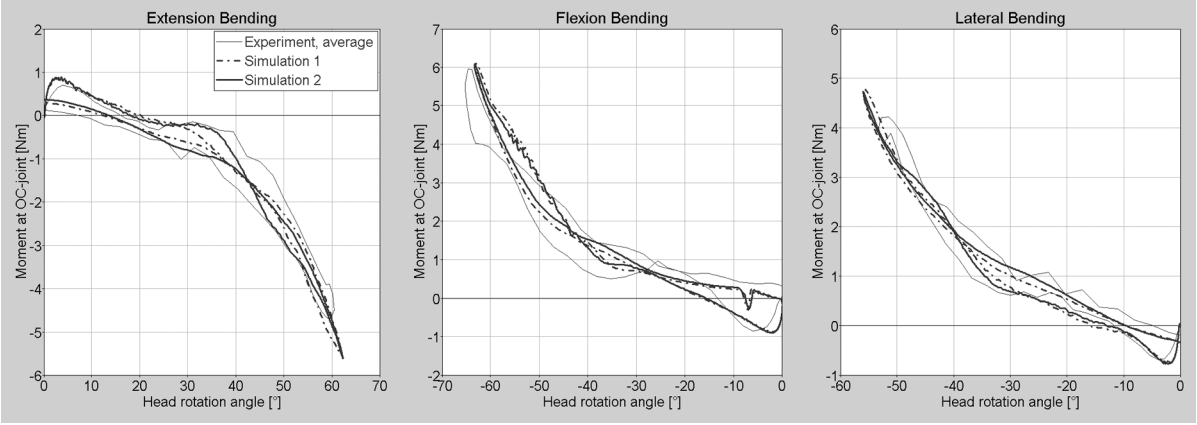

Figure 6: Neck response in sled tests.

5.2.2 Pendulum tests

The response of the neck models, validated only by using the sled tests, is already close to the results of the neck pendulum tests. Solely the head rotation differs significantly from the requirements. The validation started by varying the stiffness of the neck cable and was extended by including of the rubber material of the neck.

Figure 7 shows the response of the neck in all three bending modes. The model of the neck complies with the experimental data under extension loading up to 40°. Above this bending angle the model as well as the dummy leaves the biomechanical corridor [6]. However, both models of the neck meet the certification requirements. There is no significant difference between the two models of different grades of detail (Simulation 1 and Simulation 2).
The results of the shown neck models are also in flexion bending very close to the experimental data. Solely at an rotation angle of 65° to 70° the model leaves the biofidelity corridor. However, the certification corridor at 50° is met by both numerical models.
The quality of the neck's response in lateral bending is similar to the extension test. Above an angle of approximately 40° the model tends to be too stiff. The results of the detailed neck model are again slightly worse than the results of the less detailed one. However, both models fulfil the requirements of the certification test.

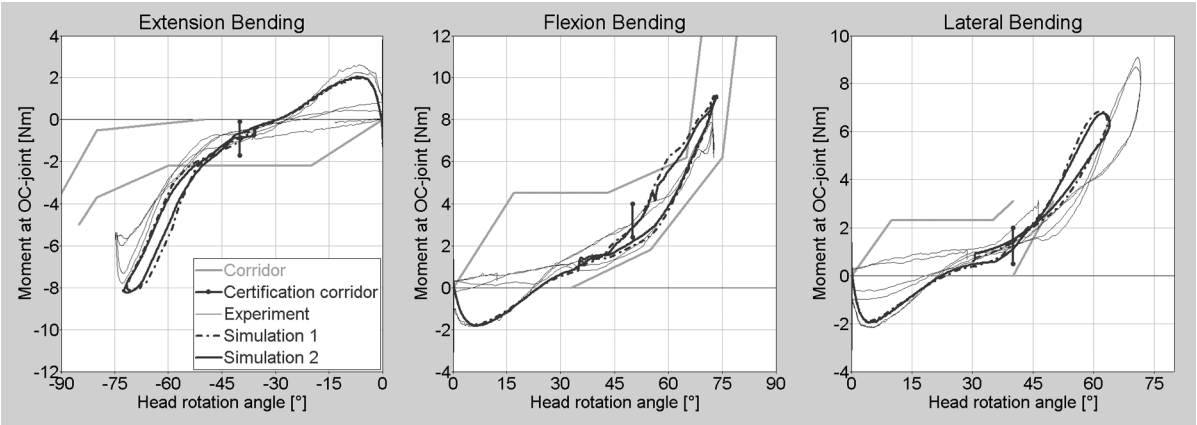

Figure 7: Neck responses in pendulum tests.

The neck was also validated to have good correlation experiment and simulation of the neck tension force F_z. The deviation to the peak values in the experiments differs up to 10% in flexion and extension bending and 20% in lateral bending.

A decision, what neck model will finally be used for the dummy model has not been made yet. The final selection depends on the results of additional tests to check the numerical robustness of the model and the head and neck response simulations using the complete dummy.

5.3 Thorax

The torso foam was pre-validated by using data of drop tests. Different types of foam models were tested. Finally material MAT_083, a Fu-Chang foam [5], was chosen. This material model is also used for the abdominal block of the LS-Dyna model of the EuroSID 2 [3]. Most of the material parameters of the EuroSID foam were transferred to the Q0 model. Only the Young's modulus E, the viscous coefficient to model damping effects (DAMP) and the only two stress-strain functions were varied. Both curves are based on a simple baseline stress-strain curve (Figure 8). They differ only due to scaling the magnitude of stress.

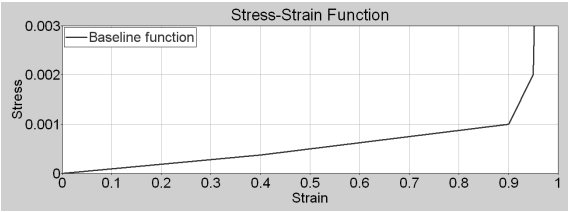

Figure 8: Baseline stress versus strain function.

The chest deflection, calculated from chest and impactor acceleration, is mainly influenced by the amplitude of the stress-strain functions and the material damping. Stiffer functions and higher damping reduces the chest deflection. At the same time the impactor force, calculated from the acceleration and mass of the impactor, increases. However, the force is mainly affected by the amplitude of the first stress-strain curve. DAMP and E have only a very small influence on the force.

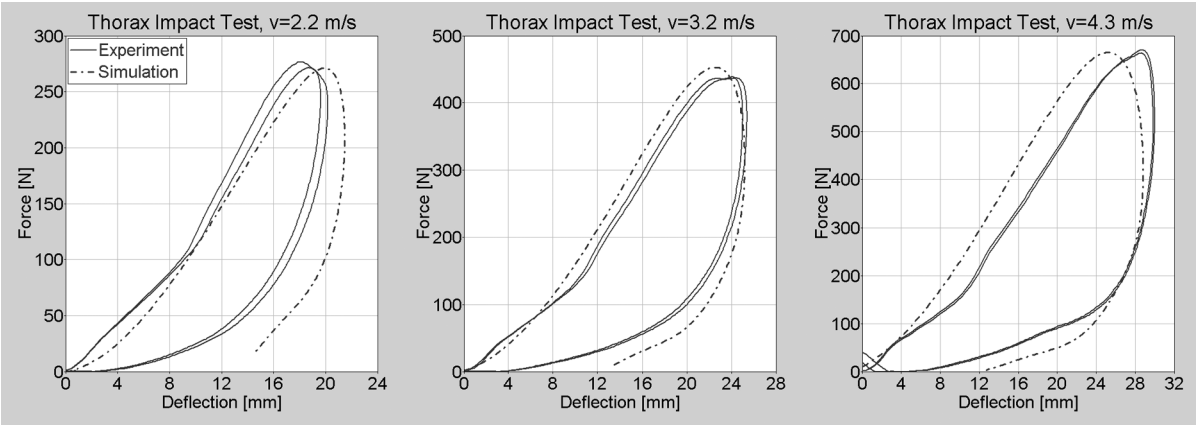

Figure 9: Force versus deflection curve different impact velocities.

Figure 9 shows the force-deflection characteristic of the torso foam at different impact velocities. The foam is slightly too soft at an impact speed of 2.2 m/s. Especially the force during the first 10 mm of chest deflection is too low. At an impact speed of 3.2 m/s the chest-deflection characteristic in the model is clearly closer to the experimental data. MAT_083 with the used parameters and curves is obviously not able to reproduce the velocity dependent effects of the torso foam correctly. The results of the impact test at 4.3 m/s supports this assumption. The foam is too stiff under these conditions. A third stress-strain function did not improve the results.

Due to some numerical problems of the torso's FE-mesh in the first simulation with the Q0 and a CRS, the mesh of the torso foam had to be modified. One of the side-effects was a reduction of the computing time of this part.

5.4 Extremities

Arms and legs of the Q0 dummy are made of the same material. So the same material model with the same properties was chosen for arms and legs.

The linear visco-elastic material MAT_006 was chosen for the extremities. The maximum acceleration of the impactor is mainly influenced by GI and BETA. An increasing GI and a decreasing BETA stiffen the material and the acceleration declines.

Figure 10 shows exemplarily the results of the arm and leg drop test with a velocity of 3.2 m/s. The simulation of the arm test correlates to the experiment in this configuration as well as in the other two with different impact velocities.
The maximum acceleration of the impactor with a leg mounted is too low at all three velocities tested. The deviation varies from 14% at 2.2 m/s to 5% at 4.3 m/s. One of the difficulties to validate the leg by using the results of drop tests could be the set-up of the tests. While the arm could easily be fixed with tape on the impactor plate and a large area of the arm had an initial contact to this plate, the fixation of the leg was difficult. The initial contact to the impactor plate was only to spots at ankle, knee and thigh. Therefore the position of the leg was less fixed than the arm's. So the leg was able to move during the impact and its deformation. Since there were no high speed video recordings of the tests available, the kinematics of the parts could not be compared to the simulation. It was decided to validate the extremities in first priority with respect to the response of the arm and in second priority to the leg. However, the achieved results are acceptable.

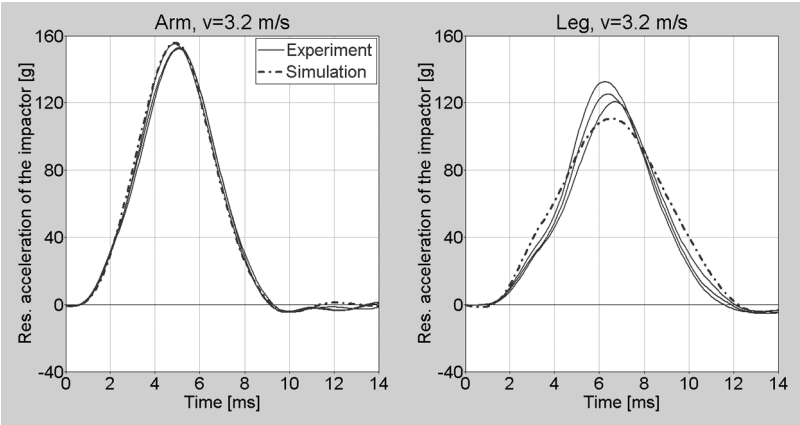

Figure 10: Acceleration in arm and leg drop test at 3.2 m/s.

Simulations, using non-linear material models to get a better velocity-dependent response, had no drastic advantage over MAT_006. The ratio between improvement of the response of the model and worsening of computing time was not acceptable.

5.5 Application of the Q0

Some frontal impact simulations were done with a generic group 0+ child restraint system and a 3-point harness to tests functionality of the dummy model (Figure 11). Initially it was difficult to place the dummy in this generic CRS. An improved model of the CRS includes a special inlay for new-born babies. The seating position of the dummy will then be more realistic.

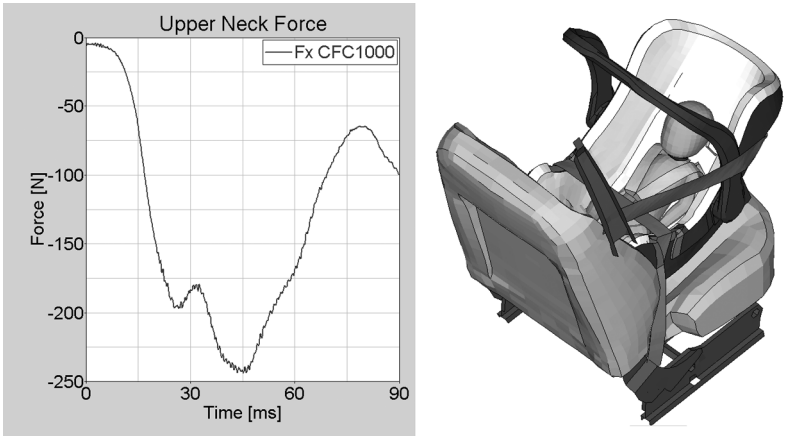

Figure 11: Q0 in a infant carrier and results of a frontal impact.

The current version of the dummy is numerical stable up to high EuroNCAP crash pulses after a redesign of the mesh of the torso foam. Especially the area of shoulders and upper back are sensitive against higher contact forces. Due to the geometrical boundary conditions of the torso foam, the elements are small in these areas and tend to collapse in the first version of the dummy.

The head acceleration and the upper neck loads show high-frequency oscillations, exemplarily shown at the shear force F_x in Figure 11, most likely caused by the load cell beam. The corresponding material parameters will be modified to obtain responses of better quality.

6 Limitations

Until now the dummy is made of validated sub-parts. The thorax impactor test was the only test with all assembled body segments and their interior contacts. All achieved results are promising and the remaining problems seem to be solvable. However, the Q0 dummy model was so far not tested in a validated CRS environment and numerical stability limits of the model are unknown at the moment. So it may be possible that some parts have to be modified in the next phase of the dummy development.

7 Further development

There is some work left to complete the development of the LS-Dyna Q0. Primarily, the dummy has to be intensely used in a CRS environment. The preparation of the modified model has already begun to run simulations with different group 0+ CRS and different seat benches. Results of corresponding experiments are already available.
The response of the head and the torso foam, and quality of the signals of some measuring points will be improved in a future step.

In parallel the model will be tested to obtain the limitations of the model in terms of numerical stability and the validation process.

8 Conclusion

The current state of the Q0 LS-Dyna model already shows a good correlation to the Q0 hardware version. All non-deformable body segments were validated by using different test set-ups or different levels of loading. So the response of the dummy segments is not only valid for a single type of loading or impact.

The resultant peak acceleration of the head is within the range of the results of two of three head drop tests. It deviates from the minimum required level by 8% in one of the three drop tests.
The neck response in flexion, extension and lateral bending is already close to the results of experiments using a pendulum and a sled test set-up, respectively.
The extremities were validated by again using a drop test configuration. The correlation of the model's response to the experiment is acceptable as there are no requirements in the certification procedures of the dummy. There is no intention to modify the achieved level of validation.
The torso foam was validated by using results of impactor tests with the complete dummy. The overall performance of the model in terms of kinematics and response of the dummy sensors is more than acceptable.

The current version of the Q0 dummy model is ready for the use within the "CHILD" project. It is needed for some in-depth studies of dummy kinematics and some parametric studies to support the experimental task of the project.

9 Acknowledgements

The development of the Q0 dummy model is part of the project "CHILD" (G3RD-CT-2002-00791) and is founded by the European Commission. More information is available on the official website of the project http://www.childincarsafety.com.

The authors would like to thank TNO Automotive and FTSS Europe for supporting the work with the provision of CAD data, results of component tests and a Q0 prototype.

10 References

[1] American Code of Federal Regulations 49, Part 572 Subpart R,

[2] American Code of Federal Regulations 49, Part 572 Subpart E

[3] Franz, U., Schuster, P., Schmid, W.: "Documentation FAT LS-DYNA ES-2 Model, Version 2.0", DYNAmore GmbH, 2003

[4] Gehre, C., Schindler, V.: "Development of the numerical model of the new-born child dummy Q0", 19th International Conference on the Enhanced Safety of Vehicles, Washington, D.C., USA, 2005

[5] "LS-Dyna - Keyword User's Manual", Livermore Software Technology Corporation, April 2003, Version 970

[6] Waagmeester, C. D.: "Q0 Dummy User's Guide", TNO Automotive, January 23rd, 2003